

GA-A25060

APPLICATION OF ELECTRON CYCLOTRON CURRENT DRIVE ON ITER

by
R. PRATER

MAY 2005

DISCLAIMER

This report was prepared as an account of work sponsored by an agency of the United States Government. Neither the United States Government nor any agency thereof, nor any of their employees, makes any warranty, express or implied, or assumes any legal liability or responsibility for the accuracy, completeness, or usefulness of any information, apparatus, product, or process disclosed, or represents that its use would not infringe privately owned rights. Reference herein to any specific commercial product, process, or service by trade name, trademark, manufacturer, or otherwise, does not necessarily constitute or imply its endorsement, recommendation, or favoring by the United States Government or any agency thereof. The views and opinions of authors expressed herein do not necessarily state or reflect those of the United States Government or any agency thereof.

GA-A25060

APPLICATION OF ELECTRON CYCLOTRON CURRENT DRIVE ON ITER

by
R. PRATER

This is a preprint of a paper to be presented at the 3rd Technical Meeting on Electron Cyclotron Resonance Heating Physics and Technology for ITER, May 2-4, 2005, Como, Italy, and to be published in the *Proceedings*.

Work supported by
the U.S. Department of Energy
under DE-FC02-04ER54698

GENERAL ATOMICS PROJECT 30200
MAY 2005



Application of Electron Cyclotron Current Drive on ITER

R. Prater

General Atomics, P.O. Box 85608, San Diego, California 92186-5608, USA

prater@fusion.gat.com

Abstract. The TORAY-GA code has been used to calculate the effectiveness of electron cyclotron waves for applications on the International Tokamak Experimental Reactor (ITER) using the steerable launchers of the reference design. This study focuses on the effect on the electron cyclotron current drive of operation of ITER over a range of toroidal magnetic field B_T from 2.35 to 5.3 T. For B_T above 4.3 T and for B_T near 2.6 T where the second harmonic takes the place of the fundamental, the launchers are satisfactory for addressing the main objectives of ECCD in ITER. Between about 4.3 T and 3.3 T, the top launcher is not usable and the midplane launchers can only be used to deposit heat near the outer part of the plasma. The applications for which the midplane launchers can be used for B_T between 3.3 T and 2.6 T depend rather sensitively on the equilibrium and the application.

1. Introduction

Plans for the International Thermonuclear Experiment Reactor (ITER) tokamak include electron cyclotron waves for heating and driving current in the plasma [1]. The key objective for electron cyclotron current drive (ECCD) is control of magnetohydrodynamic (MHD) modes like the $m=3/n=2$ and $m=2/n=1$ neoclassical tearing modes (NTMs) and sawteeth, as well as contributing to the heating to temperatures where self-heating by fusion alpha particles becomes dominant and to sustaining the current profile required for higher (“advanced”) performance in the high bootstrap fraction regime. Modeling can be employed to evaluate the power needed to carry out these objectives. The validity of the computational models used to predict the heating and current drive effects have been largely confirmed by recent experimental results worldwide [2]. In this study, the linear ray tracing code TORAY-GA [3] is used to model the current drive in ITER under a range of conditions. This code has been benchmarked extensively against experiment as well as other linear and quasilinear ray tracing and beam propagation codes.

The TORAY-GA modeling described below shows that for the reference launcher locations it may be possible to drive sufficient current density at the rational q surfaces ($3/2$ and $2/1$) of the Scenario 2 equilibrium to stabilize the neoclassical tearing mode using modulated power in the range of 20 MW and using the upper launcher, but only for a rather narrow range of optimized conditions of toroidal field for a fixed source frequency of 170 GHz. Unavoidable geometric effects place a limit on the degree to which the ECCD can be localized even if the EC beam is extremely narrow. This limit depends primarily on the launch location and the geometric relationship of the cyclotron resonance to the targeted flux surface, with the greatest localization occurring for well-collimated beams when the EC beam is traveling tangentially to the flux surface in the neighborhood of the resonance.

The fulfillment of the objectives of ECCD in ITER is greatly complicated by the range of the engineering parameters over which ITER is expected to operate. The primary objective of the ITER program is to achieve $Q=10$ in the so-called Scenario 2 equilibrium with 15 MA of plasma current and

toroidal field of 5.3 T. However, the EC system should also work with different equilibria. Cases with different profiles of safety factor q and different internal inductances have been treated by Zohm [4]. In this study, ECCD is evaluated for the upper and midplane launchers for a range of toroidal fields.

2. Approach

To test the effectiveness of the EC system for a range of toroidal fields, new equilibria were generated at the toroidal field B_T values of 4.9, 4.5, 3.6, 3.2, and 2.66 T, to scale by a factor 2 from the reference field of 5.3 T. The CALTRANS/TEQ code [5] was used to scale the equilibrium using a fixed q -profile and scaling the plasma pressure profile to keep β constant. At the same time, the density profile was scaled to keep the Greenwald number fixed. Then the EC systems were assessed computationally using the upper launcher ($R=6.485$ m, $Z=4.11$ m) and the three midplane launchers at ($R=9.076$, $Z=1.211$), ($R=9.163$, $Z=0.611$), and ($R=9.118$, $Z=0.011$). In each case, the EC Gaussian beam divergence (half angle at $1/e^2$ in power) was set to 1.08 deg to approximate the Gaussian beam size at a distance along the beam corresponding to the locations of the $q=3/2$ and $q=2$ surfaces, and the effective launch point was moved away from the final launch mirror in the direction away from the plasma by 50 cm to simulate finite beam diameter at the final mirror. It was noted that the pressure profile from the tabulated kinetic profiles for the 5.3 T Scenario 2 is inconsistent with the pressure profile from the equilibrium. In this study the density profile was derived from the equilibrium pressure profile by dividing by the sum of the tabulated ion and electron temperatures. This produced a smooth but weakly peaked density profile with a central density of $1.22 \times 10^{20} \text{ m}^{-3}$, compared to the extremely flat tabulated profile which has density $1.02 \times 10^{20} \text{ m}^{-3}$ from the center to normalized minor radius ρ of 0.93.

3. ECCD in ITER Scenario 2

The Scenario 2 equilibrium is shown in Fig. 1. The fundamental resonance intersects the two low-order rational surfaces $q=3/2$ and $q=2$ near the top of the equilibrium. The locations of the four launchers are shown as color-coded asterisks. The process followed here is to run the TORAY-GA code for a reasonable range of steering angles for each launcher to calculate the profile of driven current. An absorption model that accurately calculates absorption at both the fundamental and 2nd harmonic is used. In this study 48 rays are used in a bundle that simulates a Gaussian power distribution. The beam is characterized by poloidal and toroidal steering angles α and β , where α is the angle between the horizontal and the projection of the central ray on the plasma cross section and β is the angle between the vertical plane containing the ray and the vertical plane containing a major radius.

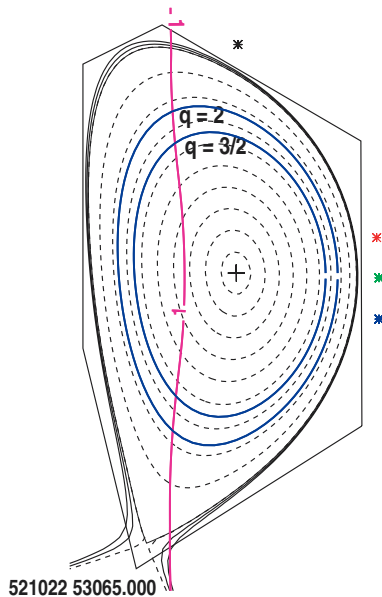


Fig. 1. ITER Scenario 2 equilibrium, with $B_T = 5.3$ T and $I_p = 15.4$ MA. The magenta vertical contour is the fundamental resonance for 170 GHz and the blue contours are the flux surfaces where $q=2$ and $q=3/2$. The black asterisk is at the location of the upper ECH launcher ($R = 648.48$ cm, $Z = 411.0$ cm) and the red, green, and blue asterisks represent the locations of the top ($R = 907.6$ cm, $Z = 121.1$ cm), middle (916.3, 61.1), and bottom (911.8, 1.1) midplane launchers.

The contours of I_{EC}/P_{EC} from ray tracing for the Scenario 2 equilibrium are shown in Fig. 2, where I_{EC} is the driven current and P_{EC} is the ECCD power, as a function of the steering angles α and β . Here, the rays are pointing more steeply downward as α becomes more negative, and the toroidal component becomes larger as β becomes more negative (β is negative because ITER requires current parallel to I_p , which is negative for Scenario 2). These contours show that the maximum current is driven for the most negative toroidal steering angles. For the $q=2$ surface, for example, the largest current of 9 kA/MW is driven at $\beta = -30$ deg. However, for this large toroidal angle the Doppler effect substantially broadens the current profile, and higher current density can be obtained at smaller β where the decrease in the profile width overcomes the decrease in the total driven current. From Fig. 3, which shows the same data as Fig. 2 except the peak j_{EC} of the driven current profile is plotted instead of the total current, the maximum current density at the $q=2$ surface of $0.5 \text{ kA/cm}^2/\text{MW}$ can be obtained for β in the range -12 to -22 deg. This can be understood from Fig. 4, which shows contours of the width of the ECCD profile, showing that $\delta\rho$ becomes smaller as β is decreased.

It is useful to see the benefits and limits of decreasing the size of the EC beam. In Figs. 5 and 6 the same calculations are shown as for Figs. 3 and 4, except that only a single ray is used. This represents the lower limit on beam size that can be accomplished through improved focusing. In fact, this unphysical limit is unattainable due to the unavoidable effects of diffraction; nonetheless, it is useful to know the current drive characteristics of a beam of zero size and zero spread in the parallel index of refraction. (Beam size and $n_{||}$ spread appear to be of comparable importance in broadening the deposition profile.) Figure 5 shows that at the $q=2$ surface, for example, the peak current density at $\beta = -20$ deg may be increased by 50% over that for the reference EC beam, but that much larger values of j_{EC} , up to $1.5 \text{ A/cm}^2/\text{MW}$, may be obtained by using smaller values of β . This may be understood from Fig. 6, which shows that very small values of $\delta\rho$, as small as 0.02, may be obtained at small values of β when Doppler broadening is dominating the profile width. For $\beta = -20$ deg, the irreducible minimum of $\delta\rho$ for any optic system is 0.04.

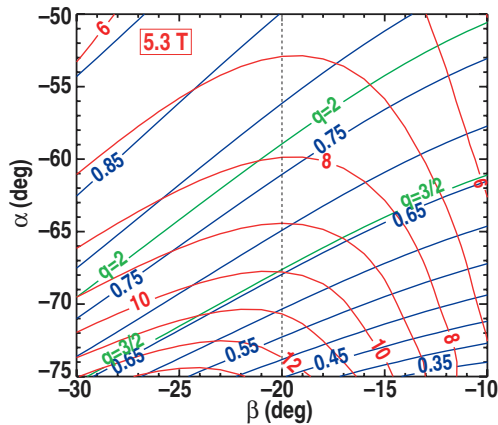


Fig. 2. Contours of the ECCD per unit power (red, kA/MW) and of the normalized minor radius where the ECCD peaks (blue), as a function of the steering angles α and β of the upper launcher for the Scenario 2 equilibrium. Also shown are the minor radius of the $q=3/2$ and $q=2$ surfaces (green). The dashed vertical line at $\beta = -20$ deg corresponds to a proposed value for fixed toroidal steering. The beam angular divergence is 1.08 deg at the $1/e^2$ power contour.

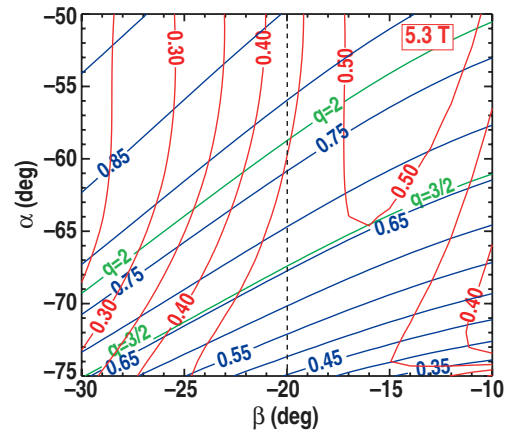


Fig. 3. Contours of the peak ECCD current density (red, $\text{A/cm}^2/\text{MW}$) for upper launcher; other information the same as for Fig. 2.

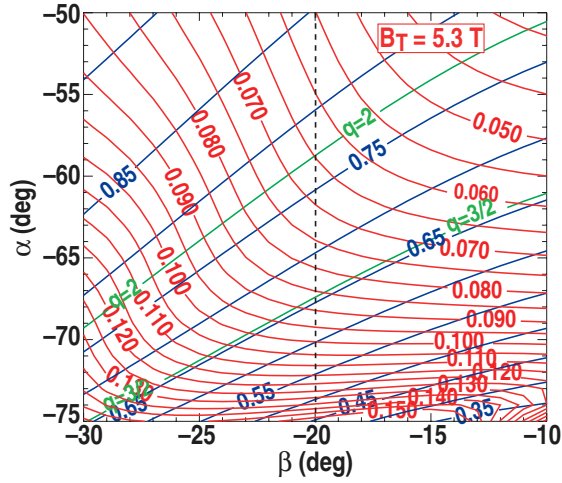


Fig. 4. Contours of the full width of the normalized minor radius at 1/e of the driven current profile (red) for upper launcher; other information the same as for Fig. 2.

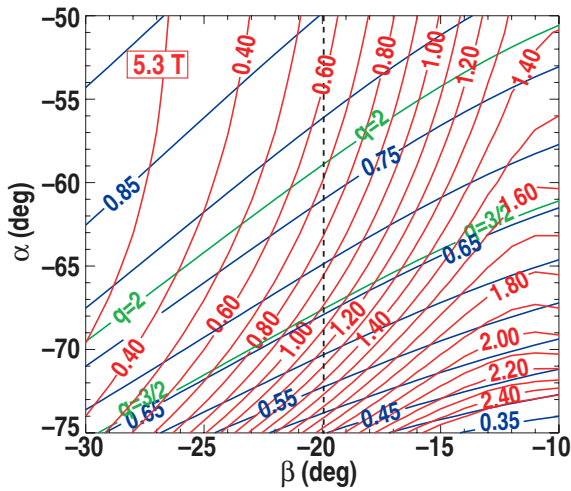


Fig. 5. Peak ECCD (A/cm²/MW); same as Fig. 3, except that zero beam divergence is used.

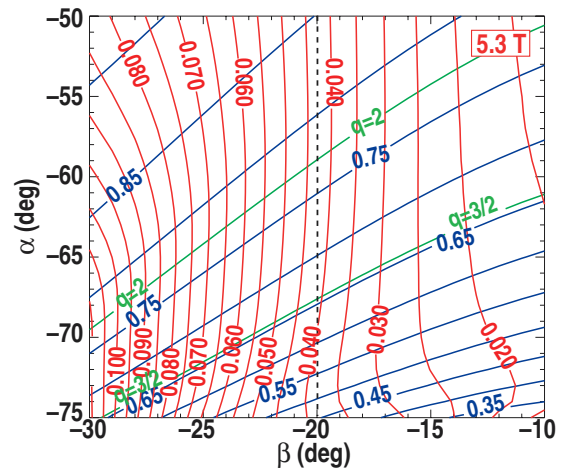


Fig. 6. Full width of ECCD profile; same as Fig. 4, except that zero beam divergence is used.

The three launchers near the midplane have fixed launching angle in the vertical direction but the steering in the toroidal direction may be varied. The results of running TORAY-GA for the range of β of -5 to -30 deg are shown in Fig. 7. For these launchers the currents are driven much closer to the plasma center than for the upper launcher, so the effects of trapping are greatly reduced and the driven currents are much larger. The middle midplane launcher is at an elevation near that of the plasma center, so only that launcher can deposit power at $\rho < 0.1$, although with a small change in α the other launchers could also. Otherwise, the power will be deposited at ρ between 0.2 and 0.4. Peak driven currents of 25 kA/MW can be obtained with these launchers, and peak current densities are above 4 A/cm²/MW.

3. ITER Scenario 2 Scaled to 4.5 T

When the equilibrium is rescaled to lower toroidal field the fundamental cyclotron resonance moves to smaller major radius, as shown in Fig. 8 for a change in B_T from 5.3 to 4.5 T. This change in geometry is favorable for obtaining high current density at the $q=2$ and $q=3/2$ surfaces since the rays now approach the resonance more nearly parallel to the flux surfaces. For the reference EC beam width the broadening of the ECCD profile is due to beam size rather than Doppler broadening, so additional

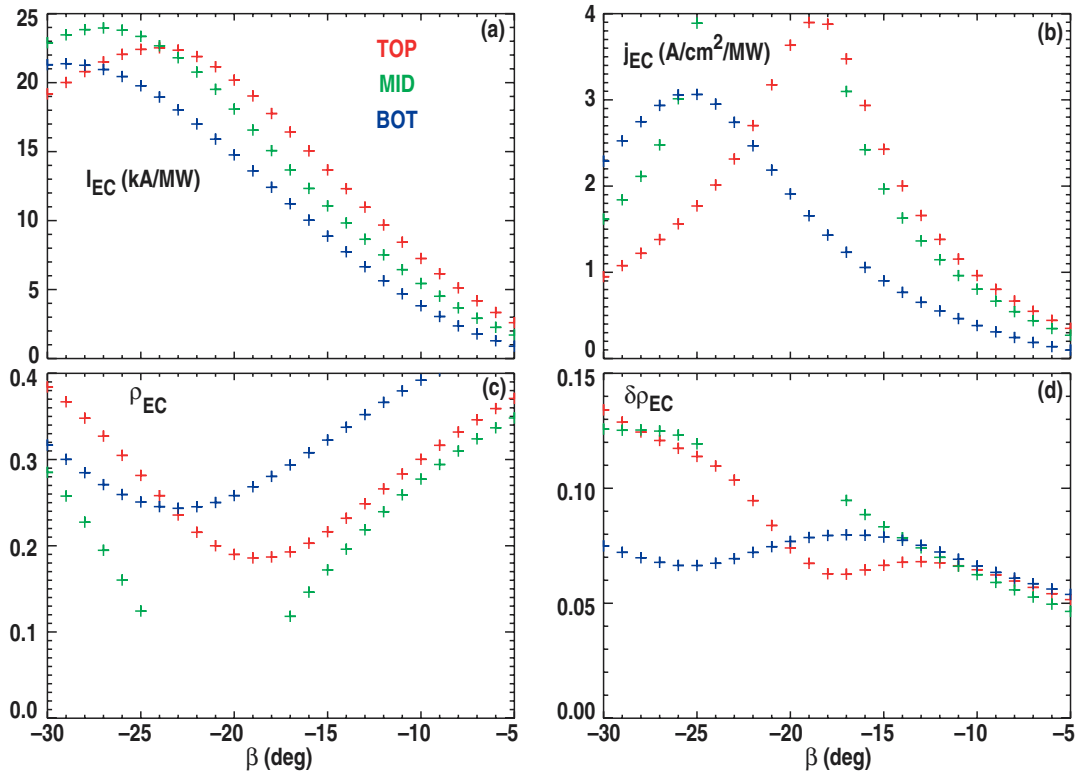


Fig. 7. Results from TORAY-GA for the midplane launchers for the 5.3 T ITER Scenario 2 equilibrium. The vertical steering angle α is 0. The top midplane launcher is in red, the middle launcher is in green, and the bottom launcher is in blue. (a) Driven ECCD, (b) peak current density, (c) normalized minor radius of the peak in the driven current, and (d) the width $\delta\rho$ at $1/e$ in the ECCD current density.

benefits may accrue from optics which produce a smaller EC beam at this location. Figure 9 shows the contours of the peak current density for this case. The value of $\beta = -20$ deg is close to the peak, which reaches $1.0 \text{ A/cm}^2/\text{MW}$, nearly double that of the equilibrium at 5.3 T. A similar increase is found for the $q=3/2$ surface. Figure 10 shows that the ECCD profile width is nearly independent of the toroidal steering angle β , supporting the conclusion that the beam width determines $\delta\rho$ and not the Doppler effect.

Varying the EC source frequency for the 5.3 T case can bring the same benefit by improving the geometry of how the wave approaches the resonance. In a previous study it was found that raising the source frequency from 170 GHz to 200 GHz produces a similar benefit, but this approach requires that the plasma be operated with full toroidal field, and any reduction in B_T causes the resonance to move outside the plasma.

At 4.5 T the midplane launchers are well suited to depositing power over the range $0.2 < \rho < 0.7$, and the peak current density is relatively high compared to that of the upper launcher for much of this range. However, the profile width is somewhat larger than for the upper launcher. This behavior is shown in Fig. 11.

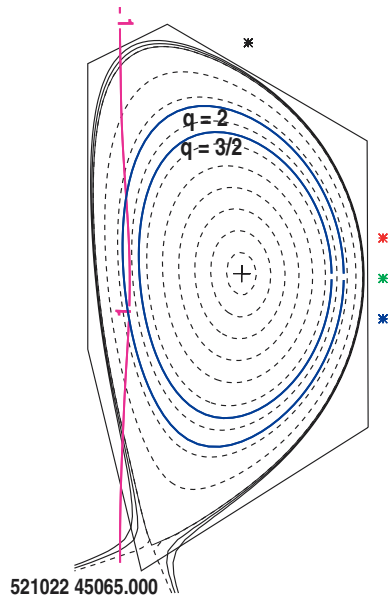


Fig. 8. Same as Fig. 1, but the equilibrium is scaled self-consistently to a toroidal field of 4.5 T.

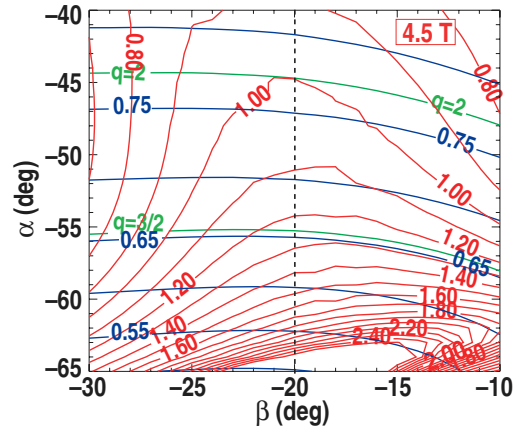


Fig. 9. Peak ECCD (A/cm²/MW); same as Fig. 3, but for the 4.5 T equilibrium.

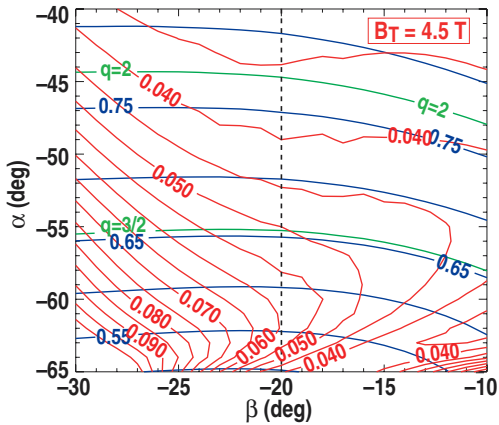


Fig. 10. Full width of ECCD profile; same as Fig. 4, but for the 4.5 T equilibrium.

4. ITER Scenario 2 Scaled Below 4.5 T

For equilibria with B_T significantly less than 4.5 T, the conditions for ECH abruptly change. For example, Fig. 12 shows the equilibrium scaled to 3.6 T. For this field the fundamental cyclotron resonance has exited the plasma on the high field side and the second harmonic has entered on the low field side. For this field the upper launcher is not usable, since access to the second harmonic is far outside the range of steering for this launcher. Even if the steering range could be increased sufficiently, ECCD using waves launched from the high field side is very inefficient due to the interaction of the resonant electrons with the trapped region of velocity space [2]. At the same time, the midplane launchers are very ineffective at driving current due to the strong canceling effects of the Fisch-Boozer current and the Ohkawa current [2]. The maximum current density for these launchers is $-0.2 \text{ A/cm}^2/\text{MW}$ (Ohkawa current dominating) at ρ near 0.95. The midplane launchers can only be used for depositing heat at ρ of 0.65 or larger.

For equilibria near 3.2 T, the applicability of the midplane launchers is improved. The equilibrium is shown in Fig. 13. Again, the upper launcher is not usable. The characteristics of the midplane

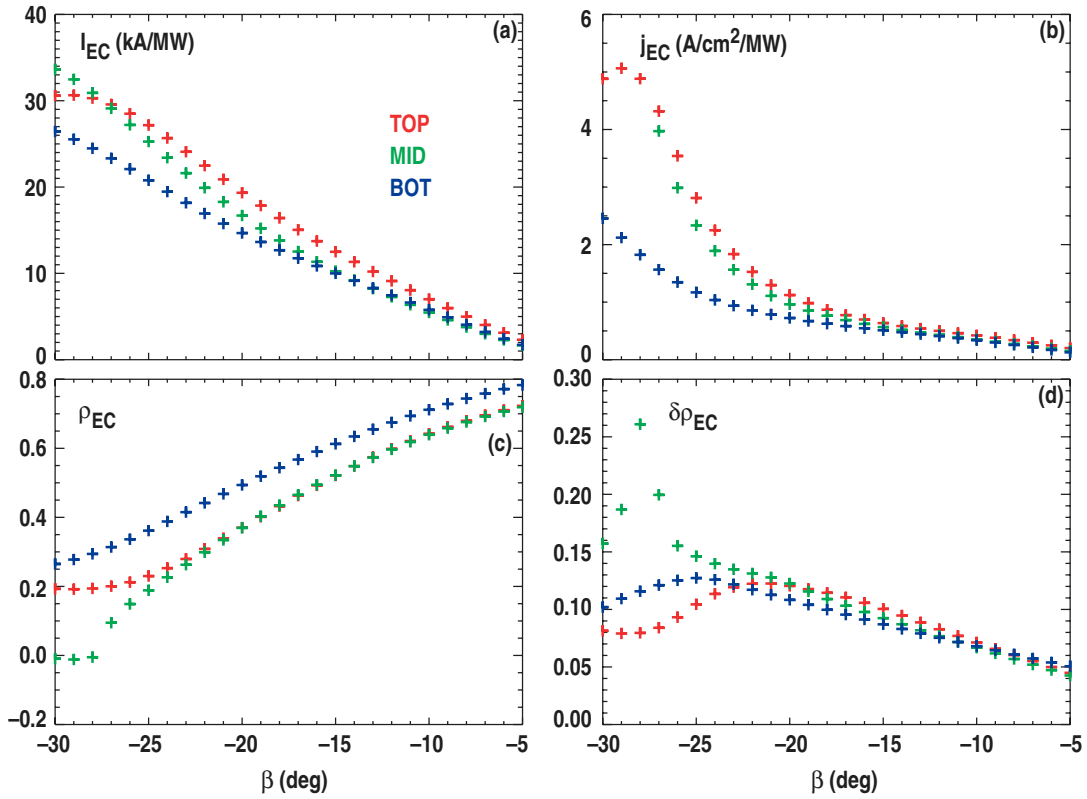


Fig. 11. Same as Fig. 7, but for the 4.5 T equilibrium.

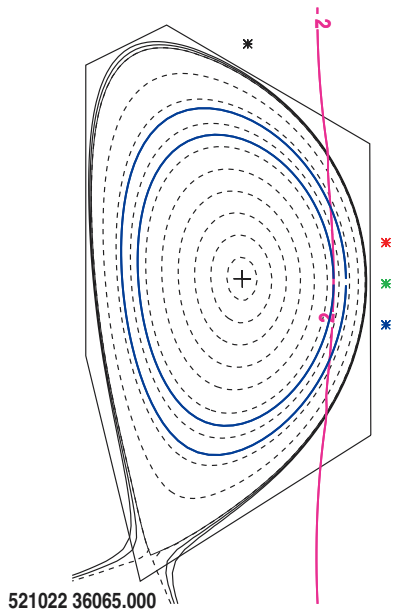


Fig. 12. Same as Fig. 1, but the equilibrium is scaled self-consistently to a toroidal field of 3.6 T.

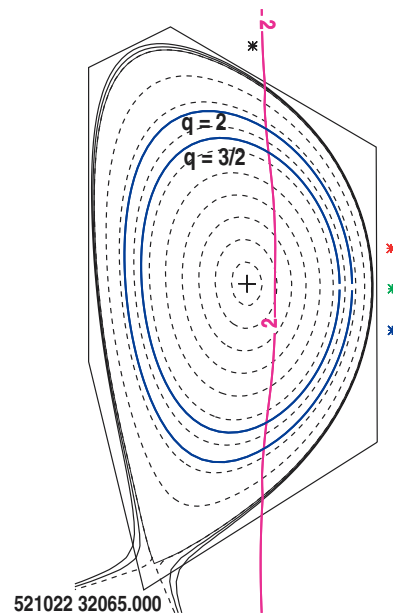


Fig. 13. Same as Fig. 1, but the equilibrium is scaled self-consistently to a toroidal field of 3.2 T.

launchers are shown in Fig. 14. Relatively large currents may be driven by these launchers near the plasma mid-radius, but the ECCD profile width is around 0.08. ECCD at minor radius in the range useful for NTM suppression can be obtained at β in the range -25 to -40 deg, but the profile width is greater than 0.1 so the peak current density is less than $0.3 \text{ A/cm}^2/\text{MW}$.

The case analogous to the 5.3 T case can be obtained at half the field. For 2.65 T, the equilibrium looks identical to that of Fig. 1 except that the second harmonic resonance replaces the fundamental resonance. The peak driven current densities are a little smaller than those of the 5.3 T case and the profile widths are a little greater.

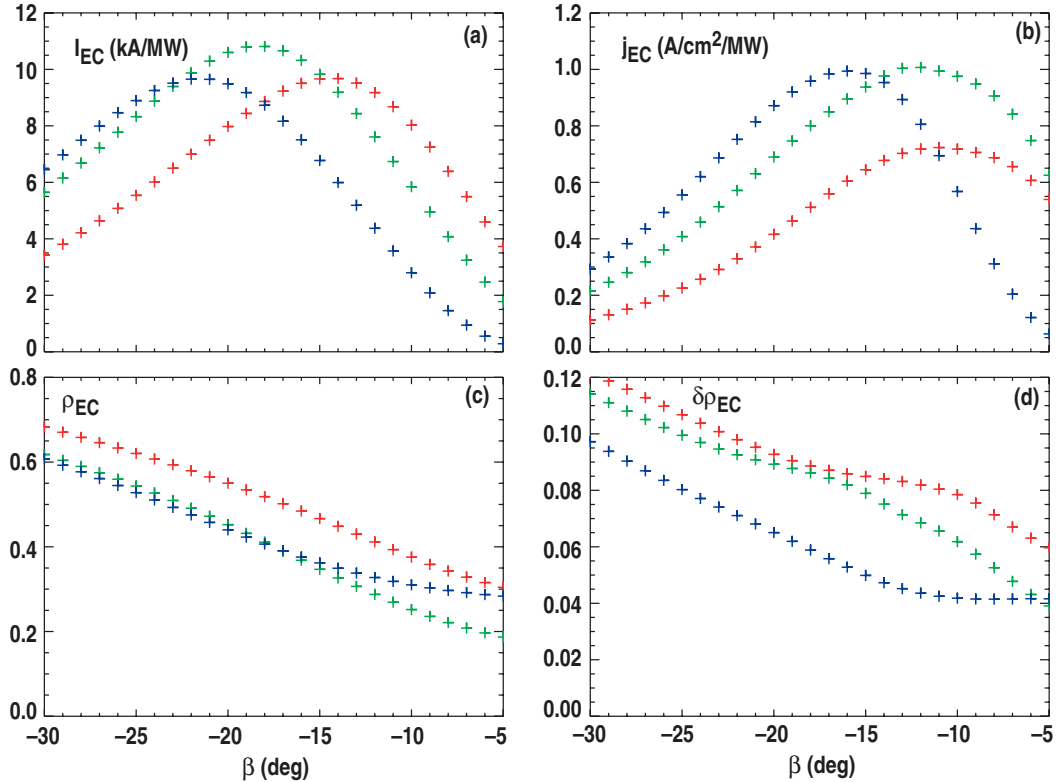


Fig. 14. Same as Fig. 7, but for the 3.2 T equilibrium.

5. Discussion and Conclusions

The upper launcher is useful for driving current for control of NTMs when the toroidal field is larger than about 4.3 T or in the range $2.15 \text{ T} < B_T < 2.65 \text{ T}$ if the second harmonic is used. The current drive efficiency is such that about 12-16 MW of EC power would be required to control each NTM based on extrapolation from experiments on ASDEX Upgrade, DIII-D, JET, and JT-60U [6]. However, even if the alignment of all the EC beams were perfect, the profile width is still larger than the island marginal size below which the mode is self-stabilizing, so modulated ECCD at the island O-point would be required for full stabilization [6]. At the top end of each toroidal field range, the upper launcher may also be used for driving current at the sawtooth radius near ρ of 0.4. The upper launcher is also well suited for heating near the plasma mid-radius. For toroidal fields outside those ranges, the upper launcher has no function.

At 5.3 T the midplane launchers are useful for heating and current drive inside the $\rho=0.4$, but with rather broad profiles. This would be effective for central heating and control of the central current density profile. As the field is dropped to 4.5 T, larger central current drive can be obtained. Far off-axis current drive with $0.5 < \rho < 0.7$ can be obtained by using a small toroidal steering angle with current densities approaching those of the upper launcher. If the toroidal field is reduced below 4.5 T,

there is growing importance of loss of power to the Doppler shifted second harmonic which approaches the outboard side of the plasma. At fields where the second harmonic has entered the plasma, the only option for obtaining strong heating is to shift the EC wave polarization to the extraordinary mode which will be fully damped before the wave reaches that resonance. For B_T in the range around 4.5 to about 3.4 T the midplane launchers are also not useful except for applying heat far off-axis (if that were desired). Below 3.4 T the midplane launchers become increasingly useful for driving broad current near the mid-radius, as may be needed for current profile control.

To summarize, some broad conclusions may be drawn about the operation of the launchers. The upper launcher and the midplane launchers should work effectively for B_T between 4.3 and 5.3 T and between 2.15 and 2.65 T. In this range, the midplane launchers are more useful for central power deposition while the upper launcher is better for larger minor radius. For B_T less than 4.5 T and greater than around 3.4 T, neither launcher works well. Between 3.4 T and 2.6 T, the applications for which the midplane launchers can be used are quite sensitive to the toroidal field, but the characteristics of the power and current deposition in this range can be confidently calculated.

This work was supported by the U.S. Department of Energy under Cooperative Agreement De-FC02-04ER54698.

References

- [1] ITER Physics Basis Editors, Nucl. Fusion **39**, 2137 (1999).
- [2] R. Prater, Phys. Plasmas **11**, 2349 (2004).
- [3] A.H. Kritz, H. Hsuan, R.C. Goldfinger, D.B. Batchelor, *Proceedings of the 3rd Int. Symp. on Heating in Toroidal Plasmas, Grenoble, Italy, 1982*, Vol. II (ECE, Brussels, 1982) p. 707; E. Mazzucato, I. Fidone, G. Giruzzi, Phys. Fluids **30**, 3754 (1987); Y.R. Lin-Liu, V.S. Chan, R. Prater, Phys. Plasmas **10**, 4064 (2003).
- [4] H. Zohm, Proc. 13th Joint Workshop on Electron Cyclotron Emission and Electron Cyclotron Resonance Heating, Nizhny Novgorod, Russia, 2004, p. 133.
- [5] T.A. Casper, et al., Plasma Phys. Control. Fusion **45**, 1 (2003).
- [6] R.J. La Haye, private communication (2005).